ACTA ONCOLOGICA
2021, VOL. 60, NO. 10, 1283–1290
https://doi.org/10.1080/0284186X.2021.1947523

Taylor & Francis
Taylor & Francis Group

ORIGINAL ARTICLE

Proton vs. photon radiotherapy for MR-guided dose escalation of intraprostatic lesions

Maryam Moteabbed[a], Mukesh Harisinghani[b], Harald Paganetti[a], Alexei Trofimov[a], Hsiao-Ming Lu[c] and Jason A. Efstathiou[a]

[a]Division of Radiation Biophysics, Department of Radiation Oncology, Massachusetts General Hospital and Harvard Medical School, Boston, MA, USA; [b]Department of Radiology, Massachusetts General Hospital and Harvard Medical School, Boston, MA, USA; [c]Hefei Ion Medical Center, Hefei City, China

ABSTRACT

Background: Dose escalation has been associated with improved biochemical control for prostate cancer. Focusing the high dose on the MRI-defined intraprostatic lesions (IL) could spare the surrounding organs at risk and hence allow further escalation. We compare treatment efficacy between state-of-the-art focally-boosted proton and photon-based radiotherapy, and investigate possible predictive guidelines regarding individualized treatment prescriptions.

Material and methods: Ten prostate cancer patients with well-defined ILs were selected. Multiparametric MRI was used to delineate ILs, which were transferred to the planning CT via image registration. Pencil beam scanning proton therapy and volumetric modulated arc therapy treatment plans, were created for each patient. Each modality featured 6 plans: (1) moderately hypofractionated dose: 70 Gy to the prostate in 28 fractions, (2)–(6) plan 1 plus additional simultaneous-integrated-boost to ILs to 75.6, 81.2, 86.6, 98 and 112 Gy in 28 fractions. Equivalent dose to 2 Gy-per-fraction (EqD2) was used to calculate tumor control (TCP) and normal tissue complication probabilities (NTCP) for ILs and organs-at-risk.

Results: For both modalities, the maximum necessary dose to achieve TCP $>$ 99% was 98 Gy for very high-risk ILs. For lower risk ILs lower doses were sufficient. NTCP was $<$25% and 35% for protons and photons at the maximum dose escalation, respectively. For the cases and beam characteristics considered, proton therapy was dosimetrically superior when IL was $>$4 cc or located $<$2.5 mm from the rectum.

Conclusion: This work demonstrated the potential role for proton therapy in the setting of prostate focal dose escalation. We propose that anatomical characteristic could be used as criteria to identify patients who would benefit from proton treatment.

ARTICLE HISTORY
Received 31 December 2020
Accepted 20 June 2021

KEYWORDS
Proton therapy; intraprostatic lesions; prostate cancer; focal boosting; MRI

Introduction

Despite continuous evolution of treatment options, the 10-year biochemical recurrence rates among high-risk prostate cancer patients remain substantial even after radical prostatectomy or conventional radiotherapy (up to 40 and 50%, retrospectively) [1–3]. Metastatic development (especially bone) could emerge following biochemical recurrence. The efficacy of radiotherapy (RT) for prostate cancer is strongly dependent on the delivered dose. Studies on uniform dose escalation of the prostate indicated approximately 10–15% reduction in rates of progression or biochemical relapse as a result of ~10 Gy uniform dose escalation [4–8]. However, uniform dose escalation could also be associated with increased risk of acute and late toxicities and is thus limited in application. Given that prostate cancer is a multifocal disease with often confined and localized intraprostatic lesions (ILs) with variable malignancy, focal dose escalations might be the optimal solution to improve disease control while sparing the organs at risk (OAR).

Imaging plays a key role in accurately identifying the ILs. Multi-parametric magnetic resonance imaging (mpMRI) is routine clinical practice for the detection of clinically significant prostate cancer. The relevant sequences typically include T1/T2-weighted MRI, diffusion-weighted imaging (DWI) that measures the diffusion of water molecules within the tissue, and dynamic contrast-enhanced (DCE) MRI that assesses the perfusion of contrast through microvessels. The inclusion of magnetic resonance spectroscopy (MRS) has also been investigated in some non-clinical studies to image the metabolite distribution within the prostate [9]. Previous studies have validated mpMRI with whole-mount prostatectomy specimens and have found significant correlation (sensitivity $>$70% and specificity $>$80%) [10,11], with a negative predictive value of up to 90% [12,13]. There is also growing evidence supporting the promising use of prostate-specific membrane antigen (PSMA) PET imaging for IL delineation [14].

Several clinical studies have demonstrated the feasibility of image-guided moderate boosts to ILs [15–23]. A phase 3

CONTACT Maryam Moteabbed mmoteabbed@mgh.harvard.edu Division of Radiation Biophysics, Department of Radiation Oncology, Massachusetts General Hospital and Harvard Medical School, 55, Fruit St., Boston, MA 02114, USA

Supplemental data for this article can be accessed here.

multicenter randomized clinical trial of patients with pathologically confirmed localized intermediate or high-risk prostate cancer included a standard arm ($n = 287$) receiving 77 Gy to the entire prostate and an experimental arm ($n = 284$) with a simultaneous micro boost to the ILs to 95 Gy total delivered by intensity-modulated radiotherapy (IMRT) in 35 fractions [18]. At a 55-month median follow up there was no observed increase in genitourinary (GU) and gastrointestinal (GI) toxicities in the study arm compared to the standard arm [19].

In light of such promising findings and continuing controversies regarding the benefits of proton therapy for prostate cancer, we aimed to compare focal dose escalations to ILs using state-of-the-art protons and photons in the context of therapeutic ratio. We investigated the level of largest achievable dose escalation by each modality considering the OAR toxicity constraints and studied strategies to limit rectal toxicities to enable potentially larger dose escalations for ILs closer to the rectum (in the peripheral zone of the prostate). We then evaluated the lowest clinically necessary focal dose for both modalities: the smallest boost to effectively maximize tumor control beyond which Tumor control probability (TCP) would plateau. Considering disease and patient variability, we further assessed individualized guidelines regarding the preferred treatment modality and optimal boost to serve as patient selection criteria for future clinical trials.

Material and methods

Patients, imaging, and IL definition

We included 10 patients with intermediate or high-risk prostate cancer with well-defined representative ILs. Diagnostic mpMRI was acquired for all patients as standard of clinical practice for staging purposes, even though the patients were actually treated using conventional uniform dose to the entire prostate. MR sequences included fast spin-echo T2-weighted (TR = 3000 ms, TE= 93.4 ms) and spin-echo echo-planar DWI (TR = 3000 ms, TE= 53.5 ms, pixel spacing =1.6 mm, slice thickness= 4 mm) acquired on a 3T GE Discovery MR750 scanner. Most ILs were located in the peripheral zone while a few were situated in the anterior stroma and transition zones. A summary of patient characteristics can be found in Table 1. Although patient 5 did not have a rectum, this data was included to assess dose escalation in complex-shaped ILs. The ILs were delineated by an experienced physician radiologist on T2-weighted MRI while using the fused apparent diffusion coefficient (ADC) images as guidance. The IL contours were consequently transferred onto the planning CT *via* rigid ($n = 6$) or deformable image registration ($n = 4$). Deformable registration was used in cases where the substantial difference in prostate shape was seen between MRI and CT, and was accomplished using Plastimatch software [24], by matching the prostate gland contours and the neighboring bony landmarks between the image pair (see Figure 1). To assess the possibility of sparing the rectum through the application of hydrogel spacers, especially important for ILs in the peripheral zone, we modeled hypothetical 7 mm thick (average in our institution) spacers by uniformly translating the rectum posteriorly for all patients.

Treatment planning

Proton and photon treatment plans were created and 6 planning scenarios were investigated for each patient: moderate hypofractionation with a uniform dose of 70 Gy to the entire prostate and 50.4 Gy to the seminal vesicles (SV) in 28 fractions, and 5 plans with the same base dose but added simultaneous integrated boost for a total dose of 75.6, 81.2, 86.8, 98 and 112 Gy to the ILs, chosen as even increments of dose-per-fraction. All plans were deliverable. Clinical Target Volumes (CTV) included prostate and prostate plus proximal SVs, and Planning Target Volumes (PTV) were created by expanding the corresponding CTVs by 5 mm (4 mm posterior). The ILs were isotropically expanded by 2 mm to create the focal PTVs, used as a boost target during treatment planning. This margin was found adequate given the high accuracy of IL identification (IL $>$ 0.5 cc), treatment robustness, and considering the consequent dosimetric tradeoffs (i.e., overdosing OAR outweighs the risk of underdosing ILs given the standard 70 Gy baseline dose), consistent with previous studies [25,26]. The urethra was delineated on the T2W images.

Proton plans were generated using the Astroid v2 treatment planning system [27–29]. A fixed relative biological effectiveness (RBE) of 1.1 was used. Bilateral opposed beams with single field optimization (SFO) were applied to ensure adequate plan robustness with respect to the proton rangeuncertainty. The spot size was ~3 mm median sigma at the relevant beam range (18–30 cm) at the isocenter in the air as achievable on our synchrotron-based gantry. The spot spacing was set to 0.8 sigma and layer spacing to 0.8 times the width of the most distal Bragg peak at 80% dose. Robustness to range uncertainties was confirmed by performing dose recalculations after ±3.5% rescaling of the HU

Table 1. Patient-specific anatomy characteristics.

Patient	Prostate volume (cc)	IL volume (cc)	IL location in prostate	Bladder size at simulation (cc)	Closest distance between IL and rectum (mm)
1	49.7	1.21	Post. left	516.46	2.4
2	26.3	2.34	Ant. left	233.62	15.9
3	67.8	4.04	Ant. left	336.77	15.4
4	65.6	1.25	Post. right	126.68	2.6
5	45.9	3.76	Center	473.18	Ileostomy: no rectum
6	86.5	1.87	Post. right	265.46	2.1
7	59.6	0.77	Post. left	195.46	10.5
8	36.4	1.85	Post. left	250.01	1.2
9	31.1	1.5	Post. right	548.87	2.1
10	65.7	0.65	Ant. right	131.72	31.3

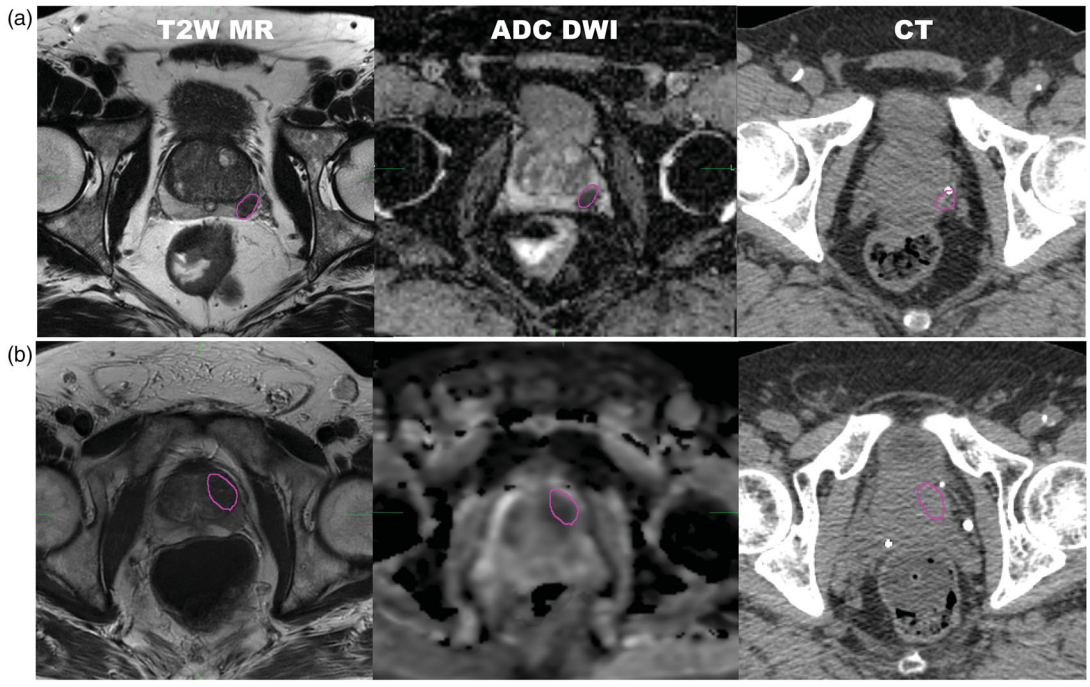

Figure 1. Intraprostatic lesions delineated on T2-weighted MRI and apparent diffusion coefficient (ADC) maps and transferred to CT for planning, for (a) patient 7 and (b) patient 3.

to relative stopping power. The photon plans were created using RayStation planning system (RaySearch Laboratories, Sweden) in volumetric modulated arc therapy (VMAT) mode with 2 full arcs with opposite rotations, 6 MV photon energy, 20 degrees collimator angle, and 0.5 cm leaf width at the isocenter.

Multicriteria optimization was used for both modalities. The dose to OARs including bladder, rectum, femoral heads, and the penile bulb was minimized similarly for both modalities. OAR constraints were adopted from an ongoing multi-institutional randomized clinical trial (see Table S1 in Supplementary material) [30]. Additionally, bladder high dose (D_{1cc}) was assessed as a measure of plan acceptability. Bladder D_{1cc} >75 Gy and D_{1cc} >80 Gy were recorded, respectively, as minor and major deviations from the constraint guidelines. The urethra was not included in the optimization, however, care was taken to keep the dose escalations highly conformal by requiring a uniform dose of 70 Gy in the prostate minus the ILs as a tradeoff objective, to spare this organ.

Tumor control modeling

The treatment response for each planning scenario was compared using the TCP model based on the concept of generalized equivalent uniform dose (EUD) [31]. EUD is a uniform dose distribution that leads to an equivalent cell kill to a given heterogeneous dose distribution (Equation (1)).

$$\mathrm{EUD} = \left(\sum_i v_i D_i^a\right)^{1/a} \tag{1}$$

Parameter a is a tissue-specific parameter ($a = -10$ for tumor and $=8$ for OARs), and v_i and D_i are bins of the differential dose-volume histogram (DVH).

This TCP formulation is advantageous because it considers the biological effect of the entire dose distribution rather than at a certain point (Equation (2)). The normal tissue complication probability (NTCP) was also based on the same formulation but with different parameter representation.

$$(\mathrm{N})\mathrm{TCP} = \frac{1}{1 + \left(\frac{\mathrm{TD}_{50}}{\mathrm{EUD}}\right)^{4\gamma 50}} \tag{2}$$

Here TD_{50} in the dose level with 50% response probability or 50% normal tissue complication probability (TD_{50} = 72.8, 77.3, 82.3, 95 Gy for low-, intermediate-, high- and very high-risk lesions, =57.3 Gy for prostate, and =80 Gy for bladder and rectum), γ_{50} is the slope of the dose-response curve (γ_{50} = 4 used for all organs) and d is the dose per fraction. The (N)TCP model parameters used were adapted from the literature [32–34]. Based on the assumption of higher clonogenic tumor density and hypoxic subvolumes, ILs were considered to be of higher disease risk than the rest of the prostate tissue and were hence assigned different TD_{50} parameters. Toxicity endpoints were contracture for bladder and grade > 2 bleeding for the rectum. The biological effect due to hypofractionation was included for all 6 plan scenarios (i.e., uniform and boosted) by replacing the dose (D) in Equation (2) by $EqD2$ (Equation (3)), which includes the linear-quadratic ratio (α/β) describing the fractionation sensitivity of each tissue ($\alpha/\beta = 1.5$ and 3 Gy for tumor and =3 Gy for OARs).

$$EqD2 = D.\left(\frac{d + \alpha/\beta}{2 + \alpha/\beta}\right) \tag{3}$$

Based on this formalism, the focal boosts applied are 90.7, 102.1, 113.6, 140, and 176 Gy $EqD2$ for $\alpha/\beta = 1.5$ Gy.

Paired-sample Wilcoxon test was used for statistical comparison of TCP and NTCP among different scenarios and modalities.

Results

Maximum achievable dose escalation

Figure 2 illustrates the dose-escalated proton and photon physical dose distributions and corresponding DVH for patients with anterior and posterior ILs (patients 3 and 4). As the DVHs illustrate, due to dose conformity, the impact of the IL boost on the OAR dose is relatively small, potentially leading to an increased therapeutic ratio for both modalities. The conformity index was comparable between modalities and independent from the level of dose escalation. The average increase in mean dose/V66 for the bladder was 1.39 Gy/0.43% and 2.10 Gy/1.33%, for protons and photons, respectively, and for the rectum 2.30 Gy/1.30% and 4.22 Gy/2.20%, respectively. The rectum mean dose was 14.2 ± 5.2 Gy for protons and 29.2 ± 3.5 Gy for photons at 98 Gy boost level. Average rectum V73.5 was 2.0 and 2.2 cc for protons and photons, respectively. The maximum increase in average mean dose for the femoral heads and penile bulb were 3.02 and 2.60 Gy for protons and 0.08 and 2.36 Gy for photons, for the largest boost. Furthermore, mean and maximum urethra doses were on average 65 Gy and 90 Gy and up to 87 Gy and 98 Gy, for the 98 Gy boost level, respectively. The average urethra mean dose was up to 2.5 Gy larger for photons than protons depending on the boost level.

The dose-escalated plans for both modalities satisfied most constraints with the exception of the maximum doses (D_{1cc}) to the rectum and bladder. Increasing the separation between the prostate and the rectum, assuming hypothetical spacers, was highly effective in reducing the rectal D_{1cc} below the clinical constraints. For protons, all other rectal constraints remained satisfied despite the increasing dose escalation. For photons, V35 showed minor deviations in a few patient cases at 98 and 112 Gy dose levels. Both protons and photons saw an increase in bladder D_{1cc} beyond the aimed dose limit. Major deviations of the bladder high dose limit were more prevalent for protons than photons for dose escalations larger than 86.6 Gy. In addition, 0 and 40% of

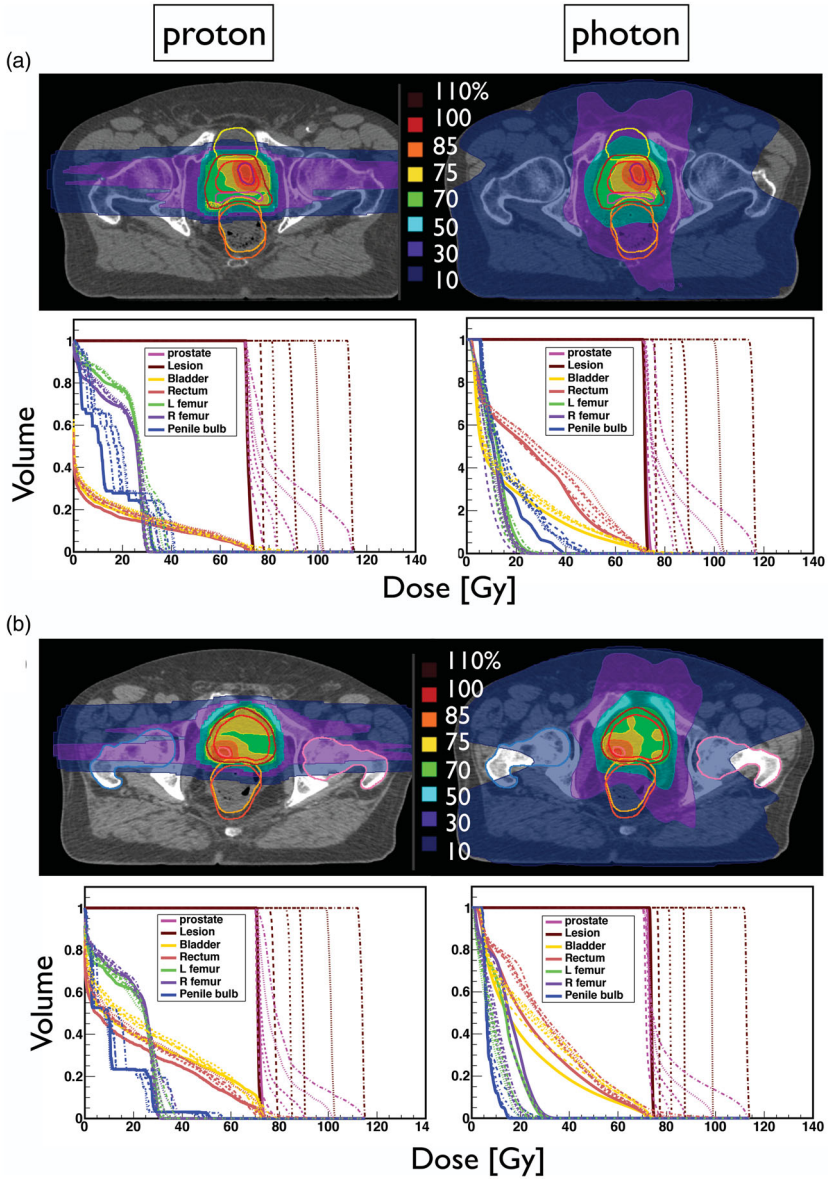

Figure 2. Proton and photon dose distributions and DVHs for example patients with (a) anterior and (b) posterior ILs.

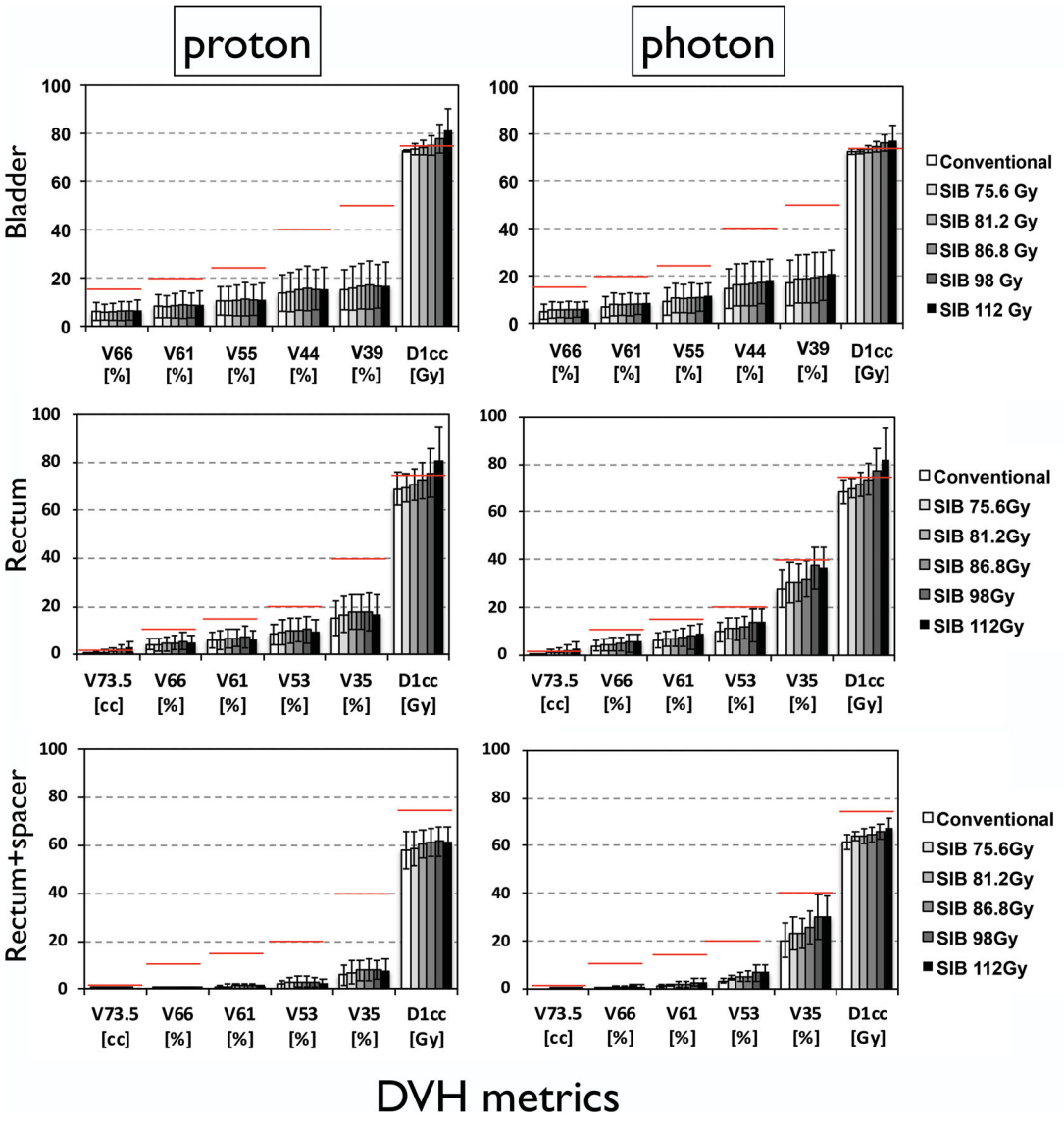

Figure 3. Comparison of DVH parameters between dose scenarios and modalities. Red horizontal lines indicate clinical protocol planning constraints.

cases exhibited minor deviations of the femoral head constraint for 98 and 112 Gy boost with protons, in comparison with 20 and 10%, respectively, for photons. Penile bulb constraint remained compliant for all escalation levels for both modalities.

Figure 3 compares the DVH metrics among dose-escalation scenarios and modalities for all OARs. It is evident that proton therapy lowers the dose at several rectal DVH points compared to photons, but in turn, photons limit the high dose to the bladder slightly better than protons. As shown before, spacers were highly effective in lowering the rectal high dose exposure in both modalities.

Biologically sufficient dose escalation

Figure 4 illustrates the effect of incremental focal dose escalation on the IL TCP and the bladder and rectum (without and with spacer) NTCP. Focal dose-escalation significantly increases the IL TCP compared to conventional plans ($p < 0.05$). Assuming tumor $\alpha/\beta = 3$ Gy, IL TCP was smaller by up to 28% compared to $\alpha/\beta = 1.5$ Gy. The TCP difference was largest for the higher IL risk group, comparable between modalities, and approached zero for larger dose escalation. As seen, the IL risk group is a clear determinant of the level of dose escalation required to achieve maximum tumor control. For both modalities, the maximum necessary dose escalation was 98 Gy to achieve >99% TCP for very high-risk tumors. Beyond this dose, no additional TCP benefit was observed, whereas the NTCP was found to continue increasing rapidly. At 98 Gy IL dose escalation, the median/maximum bladder NTCP was 8.43/19.98% for protons and 7.25/20.71% for photons, respectively. For the rectum, the median/maximum NTCP was 9.56/25.08% for protons and 10.13/35.52% for photons, respectively. When using spacers, the median/maximum rectal NTCP significantly decreased ($p < 0.05$) to 0.15/0.38% and 0.71/2.65% for protons and photons, respectively. The group difference between proton and photon NTCP was not significant for bladder ($p = 0.23$) and rectum ($p = 0.16$).

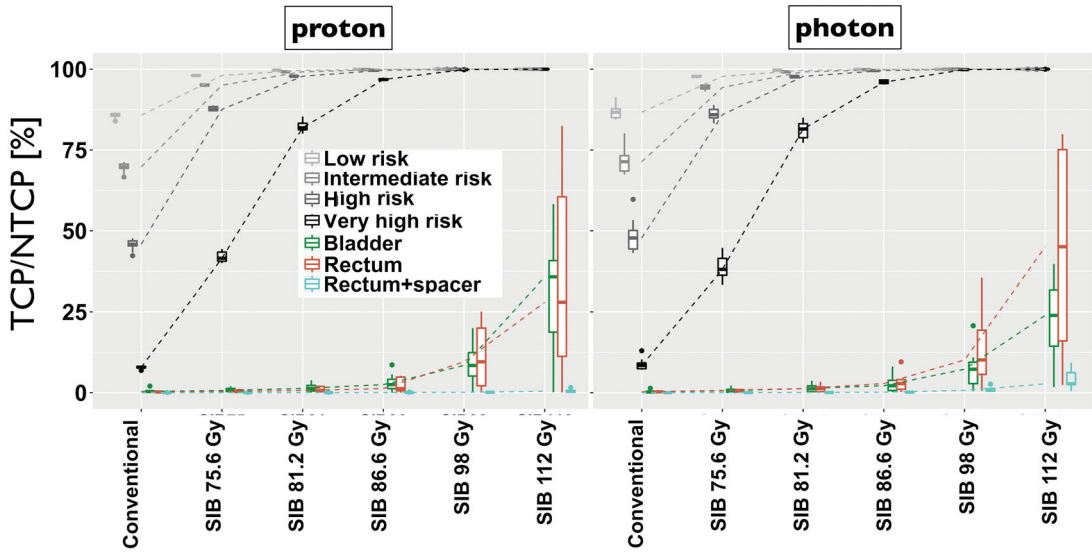

Figure 4. Comparison of IL (with different risks levels) TCP and OAR NTCP between dose escalation scenarios and modalities. Box plots represents median (mid-line), the first and third quartiles (box limits) and the maximum and minimum of the population data (error bars).

Protons vs. photons for individualized treatment

Although the differences between protons and photons for focally boosted prostate treatments were relatively small in a group setting, some key factors were identified that could help determine the preferred individualized choice of modality. These factors were based on patient-specific anatomical characteristics, which directly affected bladder and rectal NTCP. For both modalities, bladder NTCP at 98 Gy dose escalation was found to be inversely correlated with the bladder size at simulation ($R^2 > 0.8$). The only outlier was patient 6, for whom the bladder NTCP was considerably larger for photons than protons due to the bladder shape (wrapping around the prostate). In practice, a very large bladder size (>400 cc) might not be easily reproducible daily, which would contribute to inter- and intra-fractional variability and uncertainty in the delivered dose to the bladder and other organs. All patients with ILs in close proximity to the anterior rectal wall (<2.5 mm) ($n = 5$) featured increased NTCP and more severe violation of rectal D_{1cc} constraint and larger V73.5 (up to 1.2 cc) for photons compared to protons (see Figure S1 in Supplementary material). Even after applying spacers, minor deviations in rectal V35 persisted in case of VMAT for dose escalations ≥98 Gy, for 2 patients, one with the largest IL volume (patient 3) and the other with very large prostate volume but IL close to the rectum (patient 6).

Discussion

In this study, we explored the potential of proton and photon radiotherapy in the setting of mpMRI-guided focal dose escalations of ILs. As expected, we observed increased challenges meeting planning constraints when escalating the dose, especially in the bladder and rectal high dose (hot spot) region (D_{1cc}). Considering only low, intermediate, and high-risk disease, dose escalations of, respectively, 75.6, 81.2 and 86.6 Gy would be sufficient for both modalities. We found the maximum necessary dose escalation to be 98 Gy for all patients studied, yielding TCP > 99% for all disease risks (including very high-risk) and maximum NTCP < 35%. Hence, a dose escalation of 105% of TD_{50} appears to maximize the therapeutic ratio for all tumor risk groups for our specific fractionation. Considering the entire cohort, we found no statistically significant difference between modalities regarding IL TCP and OAR NTCP. However, considering individual patients, we did identify some characteristics that could guide the best choice of modality. Patients with non-standard bladder shapes, for example, prominent central lobe due to benign hypertrophy, experienced larger bladder dose with protons, whereas patients with large ILs and ones in close distance to the rectum had larger rectum NTCP for photons compared to protons. A larger sample will be needed to confirm the validity of these criteria for triaging patients between treatment modalities, which could be used as a guide in future clinical trials.

Previous planning studies have demonstrated the feasibility of moderate focal boosting to achieve better treatment outcomes than uniform dose escalation [17,25,33]. Biological optimization by varying TCP model parameters for focally boosted IMRT was found promising for improving the tumor cell kill while minimizing the OAR damage [34]. Murray et al. reported on the feasibility of boosting the ILs to 125% of the prescribed dose when utilizing a 7-fraction SBRT regimen and found rectal constraints to be a limiting factor in achieving higher escalation levels [35]. Clinical studies, for example, FLAME and DELINEATE trials have demonstrated the feasibility of boosting the ILs for moderately hypofractionated regimens and found no related excess patient toxicities [19,20]. There have been a few studies examining the role of proton therapy for prostate cancer focal dose escalation [36–40]. These studies focused on either the feasibility of using protons for dose escalation or used a single limited boost to assess the feasibility or robustness of external beam radiotherapy modalities and HDR brachytherapy to patient

variations. Our study is unique in the sense that we compared the most recent state-of-the-art proton (i.e., PBS) versus photon (i.e., VMAT) radiotherapy while determining the maximum achievable and minimum necessary dose escalation for each IL risk and identified criteria that might be helpful in making the choice between modalities depending on individualized patient characteristics.

A natural limitation of this study is that it relies on the accuracy of the biological modeling tools and parameters for calculating the TCP/NTCP. Hence, we mainly focused on comparisons between modalities rather than absolute values. We only studied bladder and rectum NTCPs for which model parameters are well established and concentrated on dose comparisons for other OARs. While the urethra dose was not specifically included in the plan optimization, the focal dose was kept conformal to minimize the high dose spill out. Urethra dose assessed post-planning was in agreement with a clinical study, which showed a similar incidence of GU toxicity between experimental and controls arms of the FLAME trial [41]. Our hypothetical use of spacers led to a relatively larger decrease (∼30%) of rectal NTCP than observed previously [42,43]. This increased effect could be attributed to the idealized approximation created by uniformly translating the rectum posterior from the prostate, while in clinical scenarios the increased organ separation created with the spacer is spatially non-uniform. Although intensity-modulated proton therapy (IMPT), and the use of beams other than laterally-opposed, could reduce the femoral head dose, we chose to use bilateral SFO proton beams with the intent to keep the plans more robust to inter- and intra-fractional variations and range uncertainty, given the acceptable dose to this OAR for dose escalations up to 98 Gy [44,45]. Although quantifying the effects of such variations is out of the scope of this study, we assume these can be minimized given the effective use of immobilization devices and the potential motion mitigation through adaptive image guidance (e.g., MRlinac). Another limitation could be relying on deformable image registration for multimodality IL contour propagation. However, recent studies have shown this could be sufficiently accurate [46]. The availability of MR-based planning could further alleviate this concern. It is worth noting that the dosimetric constraints applied in this study are relatively strict. However, the conclusions can be safely generalized across institutions independently of the constraints. Future related studies could include validating the suggested patient assignment criteria and a subsequent clinical trial to compare the outcomes of proton and photon-based dose escalation.

Conclusions

Proton and Photon radiotherapy appear equally safe and effective for focally boosted treatments of prostate cancer. Our modeling study showed sufficient tumor control and acceptable risk to the neighboring organs for even very high-risk lesions for both modalities. The physical characteristics of the lesion, prostate, and bladder might be suggestive of the preferential choice between radiation modalities.

Disclosure statement

No potential conflict of interest was reported by the author(s).

Funding

This project was supported by the Federal Share of Program income earned by Massachusetts General Hospital on [C06 CA059267], Proton Therapy Research and Treatment Center, and the Prostate Cancer Foundation.

References

[1] Artibani W, Porcaro AB, De Marco V, et al. Management of biochemical recurrence after primary curative treatment for prostate cancer: a review. Urol Int. 2018;100(3):251–262.
[2] Freedland SJ, Humphreys EB, Mangold LA, et al. Risk of prostate cancer-specific mortality following biochemical recurrence after radical prostatectomy. JAMA. 2005;294(4):433–439.
[3] Kupelian PA, Mahadevan A, Reddy CA, et al. Use of different definitions of biochemical failure after external beam radiotherapy changes conclusions about relative treatment efficacy for localized prostate cancer. Urology. 2006;68(3):593–598.
[4] Heemsbergen WD, Al-Mamgani A, Slot A, et al. Long-term results of the Dutch randomized prostate cancer trial: impact of dose-escalation on local, biochemical, clinical failure, and survival. Radiother Oncol. 2014;110(1):104–109.
[5] Zietman AL, DeSilvio ML, Slater JD, et al. Comparison of conventional-dose vs high-dose conformal radiation therapy in clinically localized adenocarcinoma of the prostate: a randomized controlled trial. JAMA. 2005;294(10):1233–1239.
[6] Peeters ST, Heemsbergen WD, Koper PC, et al. Dose-response in radiotherapy for localized prostate cancer: results of the Dutch multicenter randomized phase III trial comparing 68 Gy of radiotherapy with 78 Gy. J Clin Oncol. 2006;24(13):1990–1996.
[7] Dearnaley DP, Jovic G, Syndikus I, et al. Escalated-dose versus control-dose conformal radiotherapy for prostate cancer: long-term results from the MRC RT01 randomised controlled trial. Lancet Oncol. 2014;15(4):464–473.
[8] Beckendorf V, Guerif S, Le PE, et al. 70 Gy versus 80 Gy in localized prostate cancer: 5-year results of GETUG 06 randomized trial. Int J Radiat Oncol Biol Phys. 2011;80(4):1056–1063.
[9] Reinsberg SA, Payne GS, Riches SF, et al. Combined use of diffusion-weighted MRI and ^{1}H MR spectroscopy to increase accuracy in prostate cancer detection. Am J Roentgenol. 2007;188(1):91–98.
[10] Margolis DJA. Multiparametric MRI for localized prostate cancer: lesion detection and staging. Biomed Res Int. 2014;2014:684127.
[11] de Rooij M, Hamoen EHJ, FüTterer JJ, et al. Accuracy of multiparametric MRI for prostate cancer detection: a meta-analysis. Am J Roentgenol. 2014;202(2):343–351.
[12] Chamie K, Sonn GA, Finley DS, et al. The role of magnetic resonance imaging in delineating clinically significant prostate cancer. Urol. 2014;83(2):369–375.
[13] Itatani R, Namimoto T, Atsuji S, et al. Negative predictive value of multiparametric MRI for prostate cancer detection: outcome of 5-year follow-up in men with negative findings on initial MRI studies. Eur J Radiol. 2014;83(10):1740–1745.
[14] Goodman CD, Fakir H, Pautler S, et al. Dosimetric evaluation of PSMA PET-delineated dominant intraprostatic lesion simultaneous infield boosts. Adv Radiat Oncol. 2020;5(2):212–220.
[15] De Meerleer G, Villeirs G, Bral S, et al. The magnetic resonance detected intraprostatic lesion in prostate cancer: planning and delivery of intensity-modulated radiotherapy. Radiother Oncol. 2005;75(3):325–333.
[16] Singh AK, Guion P, Sears-Crouse N, et al. Simultaneous integrated boost of biopsy proven, MRI defined dominant intra-prostatic

lesions to 95 Gray with IMRT: early results of a phase I NCI study. Radiat Oncol. 2007;2:36.
[17] Fonteyne V, Villeirs G, Speleers B, et al. Intensity-modulated radiotherapy as primary therapy for prostate cancer: report on acute toxicity after dose escalation with simultaneous integrated boost to intraprostatic lesion. Int J Radiat Oncol Biol Phys. 2008;72(3): 799–807.
[18] Lips IM, van der Heide UA, Haustermans K, et al. Single blind randomized phase III trial to investigate the benefit of a focal lesion ablative microboost in prostate cancer (FLAME-trial): study protocol for a randomized controlled trial. Trials. 2011;12:255.
[19] Monninkhof EM, van Loon JWL, van Vulpen M, et al. Standard whole prostate gland radiotherapy with and without lesion boost in prostate cancer: toxicity in the FLAME randomized controlled trial. Radiother Oncol. 2018;127(1):74–80.
[20] Murray JR, Tree AC, Alexander EJ, et al. Standard and hypofractionated dose escalation to intraprostatic tumor nodules in localized prostate cancer: efficacy and toxicity in the DELINEATE Trial. Int J Radiat Oncol Biol Phys. 2020;106(4):715–724.
[21] Miralbell R, Mollà M, Rouzaud M, et al. Hypofractionated boost to the dominant tumor region with intensity modulated stereotactic radiotherapy for prostate cancer: a sequential dose escalation pilot study. Int J Radiat Oncol Biol Phys. 2010;78(1):50–57.
[22] Onjukka E, Uzan J, Baker C, et al. Twenty fraction prostate radiotherapy with intra-prostatic boost: results of a pilot study. Clin Oncol. 2017;29(1):6–14.
[23] Syndikus I, Cruickshank C, Staffurth J, et al. PIVOTALboost: a phase III randomised controlled trial of prostate and pelvis versus prostate alone radiotherapy with or without prostate boost (CRUK/16/018). Clin Transl Radiat Oncol. 2020;25:22–28.
[24] Sharp GC, Lui R, Wolfgang J, et al. Plastimatch an open source software suite for radiotherapy image processing. Proc. 16th Int. Conf. on the Use of Computers in Radiotherapy (ICCR), Amsterdam; 2010.
[25] Riches SF, Payne GS, Desouza NM, et al. Effect on therapeutic ratio of planning a boosted radiotherapy dose to the dominant intraprostatic tumour lesion within the prostate based on multifunctional MR parameters. Br J Radiol. 2014;87(1037):20130813.
[26] Alexander EJ, Murray JR, Morgan VA, et al. Validation of T2- and diffusion-weighted magnetic resonance imaging for mapping intra-prostatic tumour prior to focal boost dose-escalation using intensity-modulated radiotherapy (IMRT). Radiother Oncol. 2019; 141:181–187.
[27] Astroid- Proton Planning System. Available from: https://protontps.com/astroid/
[28] Kooy HM, Clasie BM, Lu HM, et al. A case study in proton pencil-beam scanning delivery. Int J Radiat Oncol Biol Phys. 2010;76(2): 624–630.
[29] Clasie B, Depauw N, Fransen M, et al. Golden beam data for proton pencil-beam scanning. Phys Med Biol. 2012;57(5):1147–1158.
[30] Efstathiou JA. Proton therapy versus IMRT for low or intermediate risk prostate cancer (PARTIQoL). 2012 [Updated 2018 Jan 9; cited 2019 Nov 8]. Available from: https://clinicaltrials.gov/ct2/show/.
[31] Niemierko A. A generalized concept of Equivalent Uniform Dose (EUD). Med Phys. 1999;26:1100.
[32] Li XA, Alber M, Deasy JO, et al. The use and QA of biologically related models for treatment planning: short report of the TG-166 of the therapy physics committee of the AAPM. Med Phys. 2012;39(3):1386–1409.
[33] Kim Y, Tomé WA. Is it beneficial to selectively boost high-risk tumor subvolumes? A comparison of selectively boosting high-risk tumor subvolumes versus homogeneous dose escalation of the entire tumor based on equivalent EUD plans. Acta Oncol. 2008;47(5):906–916.
[34] Azzeroni R, Maggio A, Fiorino C, et al. Biological optimization of simultaneous boost on intra-prostatic lesions (DILs): sensitivity to TCP parameters. Phys Med. 2013;29(6):592–598.
[35] Murray LJ, Lilley J, Thompson CM, et al. Prostate stereotactic ablative radiation therapy using volumetric modulated arc therapy to dominant intraprostatic lesions. Int J Radiat Oncol Biol Phys. 2014;89(2):406–415.
[36] Wang T, Zhou J, Tian S, et al. A planning study of focal dose escalations to multiparametric MRI-defined dominant intraprostatic lesions in prostate proton radiation therapy. Br J Radiol. 2020;93(1107):20190845.
[37] Pedersen J, Casares-Magaz O, Petersen JBB, et al. A biological modelling based comparison of radiotherapy plan robustness using photons vs protons for focal prostate boosting. Phys Imaging Radiat Oncol. 2018;6:101–105.
[38] Andrzejewski P, Kuess P, Knäusl B, et al. Feasibility of dominant intraprostatic lesion boosting using advanced photon-, proton- or brachytherapy. Radiother Oncol. 2015;117(3):509–514.
[39] Yeo I, Nookala P, Gordon I, et al. Passive proton therapy vs. IMRT planning study with focal boost for prostate cancer. Radiat Oncol. 2015;10:213.
[40] Fellin F, Azzeroni R, Maggio A, et al. Helical tomotherapy and intensity modulated proton therapy in the treatment of dominant intraprostatic lesion: a treatment planning comparison. Radiother Oncol. 2013;107(2):207–212.
[41] Van Loon J, Van Vulpen M, Pos F, et al. FLAME: influence of dose escalation to 95Gy for prostate cancer on urethra-related toxicity and QOL. Radiother Oncol. 2016;119:S24.
[42] Vanneste BGL, Buettner F, Pinkawa M, et al. Ano-rectal wall dose-surface maps localize the dosimetric benefit of hydrogel rectum spacers in prostate cancer radiotherapy. Clin Transl Radiat Oncol. 2019;14:17–24.
[43] King RB, Osman SO, Fairmichael C, et al. Efficacy of a rectal spacer with prostate SABR-first UK experience. Br J Radiol. 2018; 91(1083):20170672.
[44] Moteabbed M, Trofimov A, Sharp GC, et al. Proton therapy of prostate cancer by anterior-oblique beams: implications of setup and anatomy variations. Phys Med Biol. 2017;62(5):1644–1960.
[45] Underwood T, Giantsoudi D, Moteabbed M, et al. Can we advance proton therapy for prostate? Considering alternative beam angles and relative biological effectiveness variations when comparing against intensity modulated radiation therapy. Int J Radiat Oncol Biol Phys. 2016;95(1):454–464.
[46] Ciardo D, Jereczek-Fossa B, Petralia G, et al. Multimodal image registration for the identification of dominant intraprostatic lesion in high-precision radiotherapy treatments. Br J Radiol. 2017; 90(1079):20170021.